



The influence of experimental conditions and intermolecular interaction on the band gap determination. Case study of perylene diimide and carbazole-fluorene derivatives.



Michał Filapek*, Marek Matussek, Agata Szlapa, Sławomir Kula, Michał Pająk

Institute of Chemistry, Faculty of Mathematics, Physics and Chemistry, University of Silesia, Szkolna 9, 40-007 Katowice, Poland

ARTICLE INFO

Article history:

Received 11 April 2016

Received in revised form 7 September 2016

Accepted 7 September 2016

Available online 9 September 2016

Keywords:

Cyclic voltammetry

intermolecular interactions

arylene bisimide

carbazole

UV-Vis spectroscopy

ABSTRACT

The perylene diimide and carbazole-fluorene derivatives are intensively investigated in organic electronic and photovoltaic applications. However, they intermolecular interactions vary considerably. Herein, we present a systematic UV–vis spectroscopy and electrochemical study of intermolecular interaction influence on determination of HOMO, LUMO and band gap. The influence of this type of interactions on photophysical properties with the aid of NMR spectroscopy and DFT calculations was examined. Effect of the electrode type was investigated as well. The cyclic voltammetry results obtained at different species concentrations (including solid state measurements) were compared. We have found that when interactions are strong differences in determined band gap are significant. Contrary to half wave potential, peak onset was found to be concentration independent. Finally, we have observed that comparison of values from solid state measurement and carried out for diluted species can introduce high inconsistencies in determination of structure/property relationships.

© 2016 Elsevier Ltd. All rights reserved.

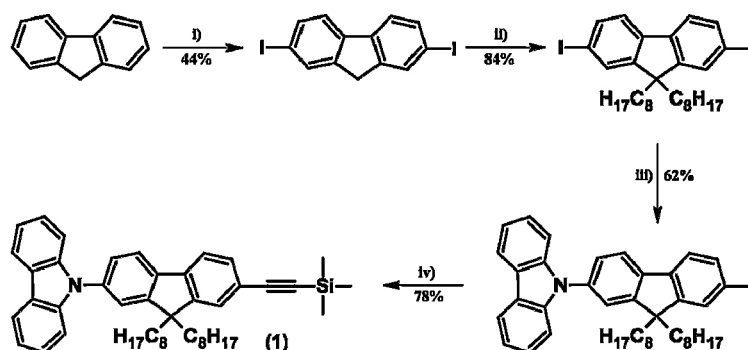
1. INTRODUCTION

Organic electronic and photovoltaic are being developed extremely fast. Progress in this field is possible thanks to structure ↔ properties feedback – in each step it is better known how the structure affects physical and chemical characteristics of the molecule and by that device performance. With that knowledge it is easier to design and synthesize compounds which have exaggerated most desired properties. However, sometimes it is difficult to compare results from different sources, especially properties related to energy levels in the molecule (HOMO and LUMO energies). This is due to the inability to measure their absolute value experimentally. On the other hand, energy values calculated by quantum chemistry methods depends on the base and functional which were used (and also by HF/DFT ratio in hybrid functional [1]). That makes those values very often only estimated. Differences between calculated and experimental values of LUMO energy are predominately especially different [2]. In contrast to HOMO, LUMO is unreal (it is empty in the real molecule which is in ground state). Furthermore, by definition of MO, that is an orbital

energy which has paired electrons (formally it would entail adding two electrons to the neutral molecule). This does not reflect the experience – electrochemical reduction the most often is a single-electron process [3], photoexcitation processes involved one electron as well. That is why sometimes radicals are analyzed using *unrestricted* DFT approach [4,5]. The ionization energy (IE) and electron affinity (EA) can be directly determined by UV-photoelectron spectroscopy (UPS) and inverse photoelectron spectroscopy (IPES). On the other hand, the most convenient (the fastest, the cheapest and very small amount of sample is needed) methods of the EA and IE determining are the electrochemical methods. Generally speaking, UPS/IPES values are larger than the values derived from CV. The offset is about 0.5–0.8 eV in case of EA and 0.4–1.0 eV for IE [6,7]. Moreover, when comparing values determined on the physical (eV) and electrode potential scales (V vs. reference electrode) in solution the potential drop across an electrical double layer (the Helmholtz layer) needs to be considered. Usually zeta potential is used for estimating the degree of this surface – solution interactions (a typical value is approximately 25–100 mV). But still there is the problem of reference calculation results to the experimental values which has been described in detail by Jean-Luc Bredas [8], P. Bujak [9], or A. Pron [10]. As mentioned before the inability to measure the absolute value of MO is the biggest problem. Because of that those

* Corresponding author at: Institute of Chemistry, University of Silesia, 9 Szkolna Str 40-006 Katowice, Poland.

E-mail address: michal.filapek@us.edu.pl (M. Filapek).



(i) I_2 , H_5IO_6 , $AcOH/H_2O/H_2SO_4$ (100:20:3 v/v), $65^\circ C$, 4h; (ii) $n-C_8H_{17}Br$, TBAB, 50% $NaOH_{(aq)}$, DMSO, $40^\circ C$, 6h; (iii) CuI , 1,10-phenantroline, carbazole, K_2CO_3 , DMF, reflux, 24h; (iv) TMSA, $Pd(PPh_3)_4$, CuI , TEA/THF, $40^\circ C$, 24h.

Fig. 1. Synthetic pathway for 1. (i) 2-ethylhexylamine, DMF, reflux, 8 h.

values have to be showed in relation to a standard, for example SCE, NHE or ferrocene [11]. It is worth to be mentioned that in literature there are different values of ionization energy of ferrocene (-4.8 eV [12], -4.88 eV [13], -5.1 eV [9]). Taking into consideration fact that this value is directly use to calculate HOMO and LUMO levels this inconsistency may hinder comparison of data from different sources.

Moreover, intermolecular interaction can also affect determination of values connected with energetic levels. Thus, we have choose compounds differing greatly in intermolecular interactions i.e. perylene diimide (exhibiting strong $\pi - \pi$ interaction between the flat aromatic sections [6]) and carbazole-fluorene (which is an amorphous substance). This paper is an attempt to systematize measurement techniques and the compare electrochemistry in solution and in the solid state with results of theoretical calculations and obtained by NMR and UV-vis spectroscopy. In addition, we examined the electrode type, scan rate and whether the sample (whether the sample is in form of solid or solution) on the obtained empirical value.

2. EXPERIMENTAL

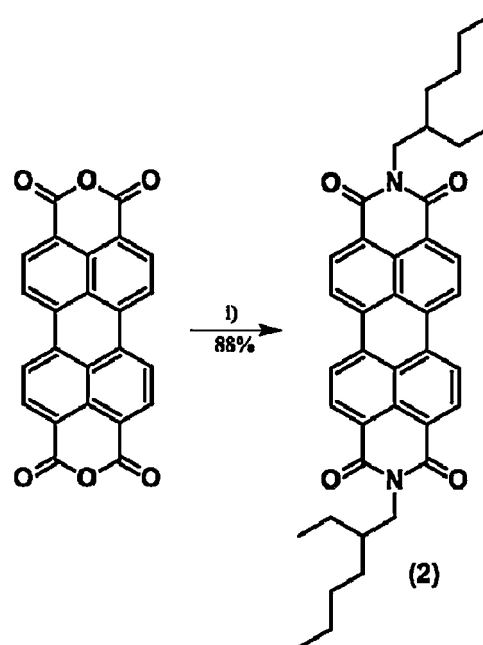
2.1. General Methods

All chemicals and starting materials were commercially available and were used without further purification. Solvents were distilled as per the standard methods and purged with nitrogen before use. Column chromatography was carried out on Merck silica gel. Thin-layer chromatography (TLC) was performed on silica gel (Merck TLC Silica Gel 60). NMR spectra were recorded with a Bruker Avance 400 MHz instrument by using $CDCl_3$ as solvent. 2,7-diiodofluorene [14], 2,7-diiodo-9,9-dioctylfluorene [15], 2-iodo-7-(9H-carbazole-9-yl)-9,9-dioctylfluorene [16], N,N'-bis(2-ethylhexyl)-3,4,9,10-perylene diimide [17] were prepared to the literature procedures. Synthesis details for 2-(trimethylsilyl)-7-(9H-carbazole-9-yl)-9,9-dioctylfluorene (**1**) can be found in SI. Both synthesis pathways are summarize in Figs. 1 and 2 for compounds (**1**) and (**2**), respectively. UV/Vis spectra were recorded with a Hewlett-Packard model 8453 UV/Vis spectrophotometer in dichloromethane solution. Electrochemical measurements were carried out with an Eco Chemie Autolab PGSTAT128n potentiostat using glassy carbon, gold, platinum (all with diam. 2 mm) or Indium tin oxide (ITO, with 10Ω per square) as working electrode. For thin film preparation, substances were spin-coated on the cleaned electrode surface from fresh solution (2 mg/cm^3 in methylene chloride (DCM)) and baked 30 min at $60^\circ C$. Platinum

coil, and silver wire were used as auxiliary and reference electrode, respectively. Potentials are referenced with respect to ferrocene (Fc), which was used as the internal standard. Cyclic and differential pulse voltammetry experiments were conducted in a standard one-compartment cell, in CH_2Cl_2 (Carlo Erba, HPLC grade), under argon. Bu_4NPF_6 (Aldrich; 0.2 M, 99%) was used as the supporting electrolyte. The quantum theoretical calculations were performed with use of density functional theory (DFT), with an exchange correlation hybrid functional B3LYP and the basis 6-311 + G(d,p) for all atoms. The calculations were carried out with use of Gaussian 09 program.

3. RESULTS

For the measurement, two compounds with very different physical and chemical properties have been chosen, although they both belong to the intensively investigated for use in organic electronics groups of compounds. Compound **1** (carbazole



(i) 2-ethylhexylamine, DMF, reflux, 8h.

Fig. 2. Synthetic pathway for 2.

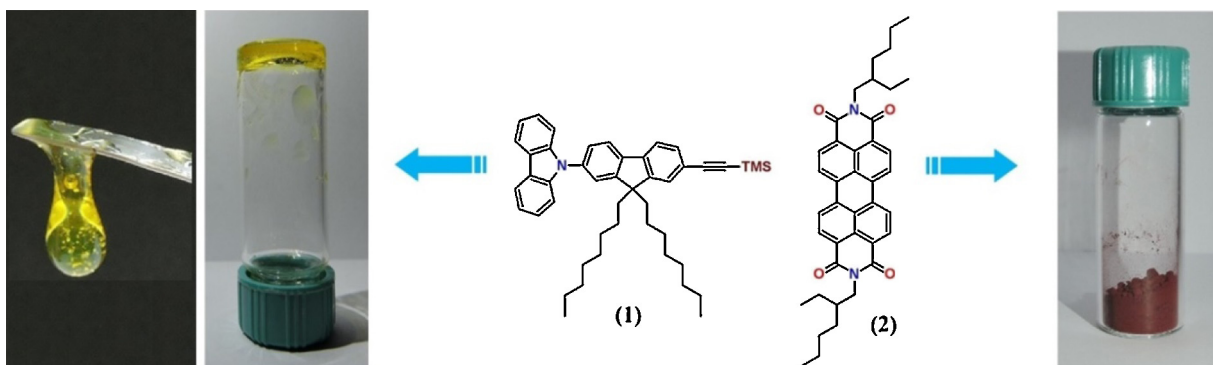


Fig. 3. The structures of the examined compounds together with photos of 1 and 2.

derivatives) is an amorphous compound with high viscosity (Fig. 3). It does not crystallize even after cooling, this suggests a very weak intermolecular interactions. Compound **2** i.e. perylene diimide (PDI) derivatives is selected from the group of compounds with the tendency to form a strong π – interaction between the flat aromatic sections [6]. This feature makes this type of compounds crystalline solids what was also observed in the case of **2** (Fig. 3).

In a first step, a series of NMR analysis of the solutions with different concentrations of the **1** and **2** have been performed. As shown in Fig. 4 aromatic hydrogen in PDI with increasing concentration become increasingly shielded. In other words, the lines of magnetic force (generated by the electrons swirling motion within the aromatic ring) are arranged in a way those hydrogens are increasingly obscured as the concentration increases (the paramagnetic effect) (Fig. 4) and thus, hydrogen atoms absorb wave of increasing energy as the concentration increases. As has been reported earlier [18] the planes of the aromatic rings tend to set in parallel (if there are no steric obstacles). This results the stronger interactions *induced dipole – induced dipole* and consequently lowers the energy of the system. On the other hand, in the case of **1** completely reverse phenomenon has been observed (see Fig. 1 S in supplementary materials). This is due to its structure – that is, nearly orthogonal two aromatic rings – carbazole and fluorene. Thus, it is impossible for the molecule to set in parallel – and this increases diamagnetic effect as the concentration increases – lines of the magnetic field are arranged in such way that counteract external magnetic field.

It is worth remembering that NMR technique directly measures the resonance frequency of the nuclei of hydrogen, but it is directly dependent on the ambient electron (electron density). Differences

between the behavior of both substances during measurements by other techniques (CV and UV- vis) should be expected.

In a further step the effect of the concentration on UV–vis spectrum has been examined. In the case of **1** the difference between the absorbance onsets in a solid and in a solution is low (a few nanometers) i.e. 360 nm (what can be recalculated to 3.44 eV using $E_g = 1240/\lambda_{abs}$ formula) in solution ($2e^{-6}$ mol/L) and 363 nm (3.41 eV) in a thin layer (Fig. 2S in supporting information). As has been previously demonstrated with a NMR technique orthogonal rings prevent the creation of strong intermolecular interactions, thus concentration has negligible influence. In case of **2** significant decreasing energy gap when the concentration increases was observed – from 536 nm (2.31 eV; for a $2e^{-6}$ mol/L solution) to 608 nm (2.04 eV for thin layer) – see Fig. 5.

A similar relation was already described for compounds having in their structure PDI moiety [6,19] – aggregation always causes an increase of absorbed light wavelength (i.e. photons with smaller energy). It should be empathizing that during UV–vis spectra measurement generation of “Frenkel exciton” occurs – excited electron remains in a Coulomb contact with a hole. Bearing in mind strong π – π interaction in PDI, holes become more stabilized by a resonance with increasing concentration. This fundamentally differentiates this technique from electrochemical measurement. It should be always concerned that during the electrochemical reduction electron is delivered “to the system” (from the electrode surface). Similarly, during the oxidation of molecule the electron is “derived” from the electrode. Therefore questionable is the method used sometimes in the literature when for the HOMO energy calculation equation: E_g (determined from uv–vis spectroscopy) –LUMO (determined from cyclic voltammetry) is used (or, similarly, for LUMO: E_g (determined from uv–vis spectroscopy)

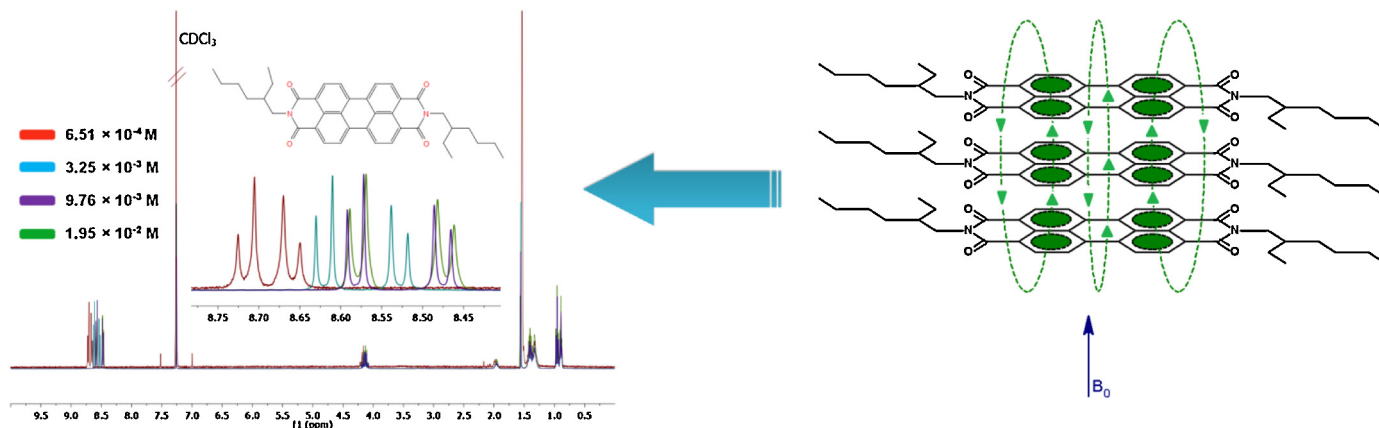


Fig. 4. ^1H NMR spectrum (depending on the concentration in CDCl_3 solution) and paramagnetic effect of **2**.

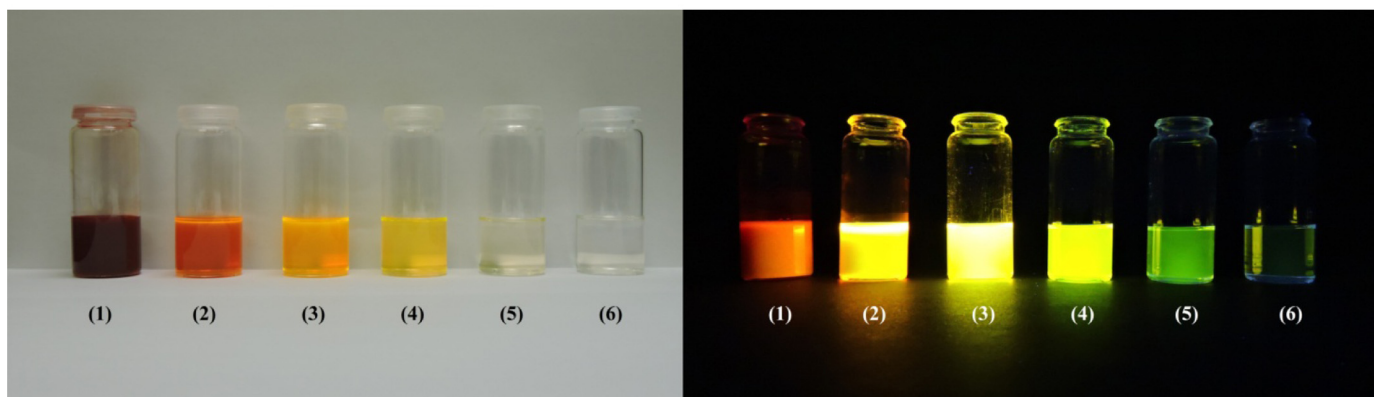
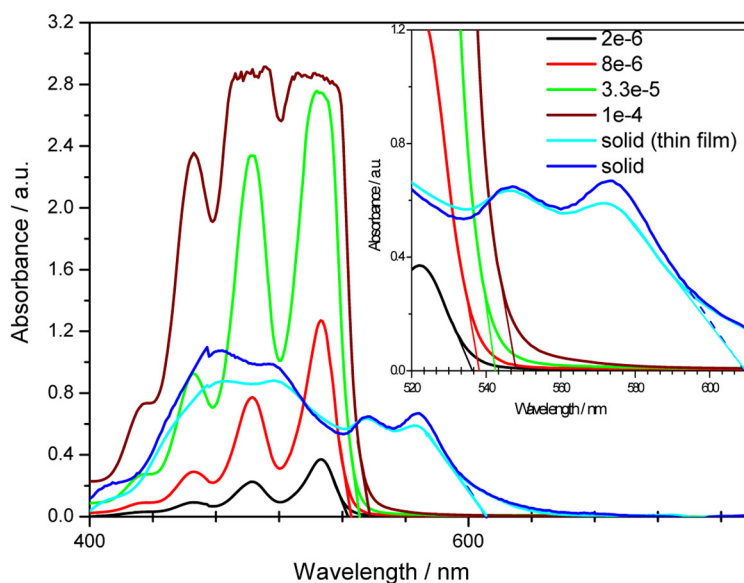


Fig. 5. UV-vis spectrum at various concentration (top) and luminescence of compound **2**, concentrations in CH_2Cl_2 solution (bottom): 1) 10^{-2} M; 2) 10^{-3} M; 3) 10^{-4} M; 4) 10^{-5} M; 5) 10^{-6} M; 6) 10^{-7} M (Left: under visible light, right: under irradiation with light at 366 nm).

—HOMO (determined from cyclic voltammetry)). Moreover, some transitions are either symmetry forbidden or has negligible oscillator strength, becomes spectroscopically inactive. On the other hand, cyclic voltammetry don't share these restrictions – electrochemical measurement is based on thermodynamics laws deriving directly from a chemical potential change and electrical work:

$$dG_i = RT \ln a_i = We = -zFE^0_{\text{R}} E = E^0 + (RT/zF) \ln(a_{\text{ox}}/a_{\text{red}}) \quad (1)$$

The last equation (1) is of course the Nernst equation. However, we have to remember that in the equation the activities of the substances are used ($a_i = f \cdot c$), not simply the concentration ($a = c$ – only for ideal solutions or ideal, dilute solutions). Secondly, the effect of electrolyte and solvent has to be considered. This issue is substantially reduced by the use of an internal standard i.e. ferrocene (assuming similar environmental shift of oxidation/reduction onsets) and using the extrapolation of the linear part of the obtained curve (for which Nernst equation is strictly fulfilled). Additionally, our experience with measurements of amide systems clearly shows that working electrode type is also important, especially in the case of measuring systems with multistage redox processes (eg. imide copolymers) [20]. Thus, electrochemical research has been begun by analyzing the impact of electrode material on the result.

For each diimide (DI) a reduction process towards the formation of an anion radical according to mechanism put forward by S.-H.

Hsiao et al. [21] was recorded, what is also in agreement with our previous research [20,22,23]. As it is shown on voltamograms above (Fig. 6) the first (i.e. PDI/PDI^-) and the second ($\text{PDI}^-/\text{PDI}^{2-}$) reductions were reversible and well detectable (except for the case

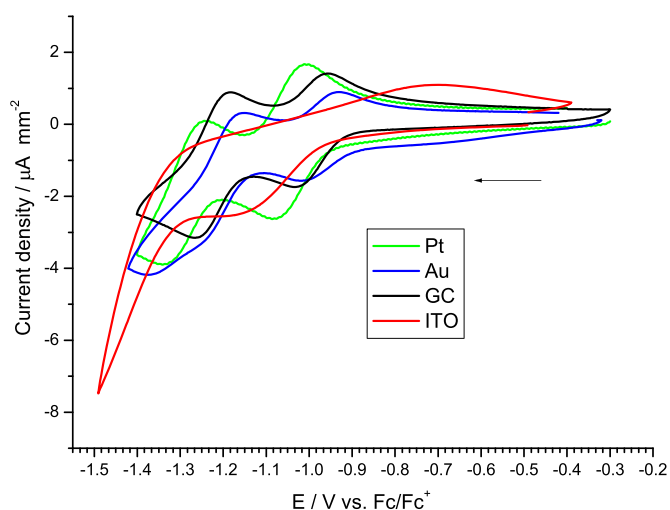


Fig. 6. Cyclic voltammograms obtained for **2** for different working electrodes; arrow shows the initial direction of current flow; $c = 10^{-5}$ mol/dm³, sweep rate $\nu = 100$ mV/s, 0.1 M Bu_4NPF_6 in CH_2Cl_2 .

Table 1

Comparison of electrochemical and theoretical data.

Code	IE ^a (CV) [eV]	EA ^b (CV) [eV]	HOMO (DFT) [eV]	LUMO (DFT) [eV]	IE ^c (DFT) [eV]	EA ^d (DFT) [eV]	Eg (DFT) [eV]	Eg (CV) [eV]	Eg (opt) [eV]
1	5.85 ^e (5.80) ^f	-2.75 ^e (-2.68) ^f	-5.79	-1.86	5.52	-2.15	3.93 ^g (3.37) ^h	3.10 ^e (3.22) ^f	3.44 ^e (3.41) ^f
2	6.29 ^e (6.41) ^f	-4.10 ^e (-3.96) ^f	-6.14	-3.68	5.94	-3.92	2.46 ^g (2.02) ^h	2.19 ^e (2.45) ^f	2.26 ^e (2.04) ^f

^a IE (eV) = |e|(E_{ox(onset)} + 5.1) measured using GC.^b EA (eV) = -|e|(E_{red(onset)} + 5.1) measured using GC.^c IE is energy change in the process M - e⁻ → M⁺.^d EA is energy change in the process M + e⁻ → M⁻ (negative values indicate exothermicity upon reduction of molecule).^e determined for solution.^f determined for solid state.^g from HOMO-LUMO.^h from |IE| - |EA|.

where ITO were used as working electrode). First reduction onsets measured for the **2** on gold and GC electrodes are almost identical (-0.99 V and -1.00 V, respectively). On the other hand, in the case of Pt electrode onset is lower by about 70 mV (i.e. -1.07 V). What is also important difference between onsets E_{1red} and E_{2red} registered on the Au and GC electrodes is as follows: 240 mV and 220 mV (so very close in value to each other), while on Pt electrode is almost 300 mV, which suggests difficulties with the charge transfer. Probably, in this case platinum complex is formed on a surface with the imide (being O-donating ligand) which impedes the flow of charge. However, in each case of the conducting electrodes processes are fully reversible from a formal point of view. As can be seen at Fig. 6 for ITO (which is semiconducting electrode) even in the solution under identical conditions processes are quasi-reversible. Moreover, onsets of the first stage of the reduction are evidently lower (E_{1red} = -1.12 V) and quasi-reversible while second become to be irreversible. For the oxidation we also observed some variations in onsets (see Table 1 S in supp. inf.). But what is important in the case of platinum and (especially) ITO electrodes the oxidation onsets were much less apparent, and this explains the fact that sometimes it is difficult to determine the oxidation potential of those electrodes (see Fig. 3 S in supp. inf.). On the other hand on GC and Au electrodes are well defined, so if there are difficulties with electrochemical measuring it should be decided to use a different type of electrode.

We have studied also the concentration affects on a band gap determined electrochemically. As it has been already reminded

previously the measured potential is dependent on the activity of a examined substance. Therefore, changing the activity (by changing the concentration) must affect on the observed potential (it changes in logarithmic segment). We have to remember that difference between the cathodic and anodic peaks |E_{pc}-E_{pa}| (peak-to-peak separation) should be 56 mV (approximately) for one electron, reversible process. Additionally, the average of this two peaks (E_{1/2}) is taken as excellent approximation of E⁰ [11] and is commonly used by many researchers. On the other hand peak onset value is also commonly used [24,25]

As shown on the voltammograms above (Fig. 7) with increasing concentration the maximum of E_{pa} is shifted by 50 mV concentrating solution 10-times (in case of **2** at 1 × 10⁻² mol/L precipitates of measured species occurs). But E_{pc} for the concerned process is nearly independent from this factor. In our opinion, this phenomenon is caused by the fact that in each case concentration of reduced form generated during measurement is approximately the same (and a_{red} as consequence). But a_{ox} is strongly depended from concentration, thus a_{ox}/a_{red} ratio is different in each time. This implies, that from the thermodynamical point of view only at low concentration process is pure reversible (|E_{pc}-E_{pa}| = 56 mV). At higher concentration process could be mistakenly assigned as quasi-reversible (for example |E_{pc}-E_{pa}| = 150 mV at 1 × 10⁻³ mol/L). However, in all cases (even in 1 × 10⁻² mol/L solution) peak onset is constant.

We have also compared the behavior of the substance in the form of solutions and the thin layer applied on the surface of the electrode. As shown at Fig. 8, the oxidation of the carbazole derivative takes place a bit easier for a solid. Furthermore, in the solution characteristic irreversible oxidation of carbazole can be registered, not fully shaped in a solid.

Much bigger differences have been observed making a similar comparison for perylene derivative (Fig. 9).

It can be easily observed that both oxidation and reduction, in this case take place much harder in the solid than in solution. In addition, the reduction is no longer a reversible process (in the pure sense thermodynamics), and become quasireversible (similar behavior was reported by A.O. Aleshinloye et al. for similar PDI derivative [26,27]). This also results in a significant diminution in “energy gap” determined electrochemically. Moreover, the difference is surprisingly high - Eg in the solution is 2.1 eV, while in the solid state is 2.4 eV. Importantly, the results are almost identical, regardless of the material of the electrode. What is interesting that the ratio of current of redox processes changes. In the case of solutions the reduce peak current (E_{1red}) is comparable to the current which flows during the oxidation (even higher during oxidation). In the case of solids the peak of oxidation is almost unnoticed when the same scale as for reduction is used. So how this difference and quasi-reversible nature of the reduction should be explained? It must be remembered that the perylene derivative is an n-type semiconductor [28]. That is why during the oxidation

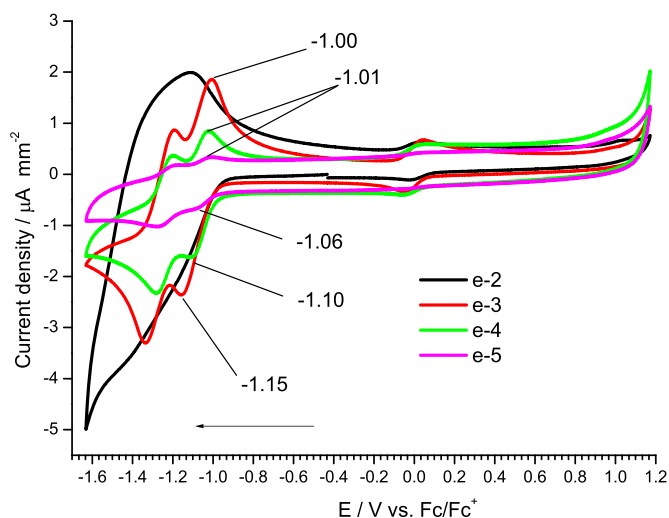


Fig. 7. Selected cyclic voltammograms obtained for **2** at different concentration, GC as working electrode, arrow shows the initial direction of current flow; sweep rate $\nu = 100$ mV/s, 0.1 M Bu₄NPF₆ in CH₂Cl₂.

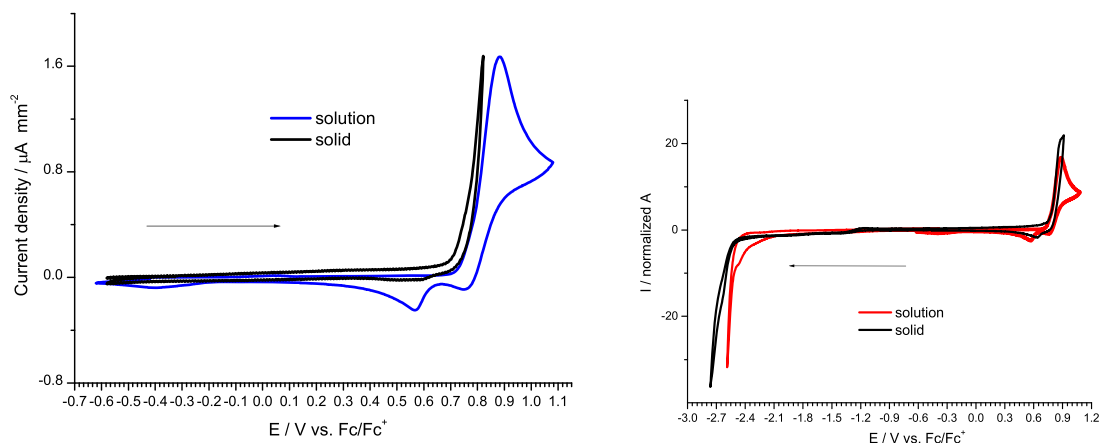


Fig. 8. Selected cyclic voltammograms obtained for **1**; arrow shows the initial direction of current flow, GC as working electrode; $c = 10^{-5} \text{ mol/dm}^3$ (for solution), sweep rate $\nu = 100 \text{ mV/s}$, $0.1 \text{ M Bu}_4\text{NPF}_6$ in CH_2Cl_2 .

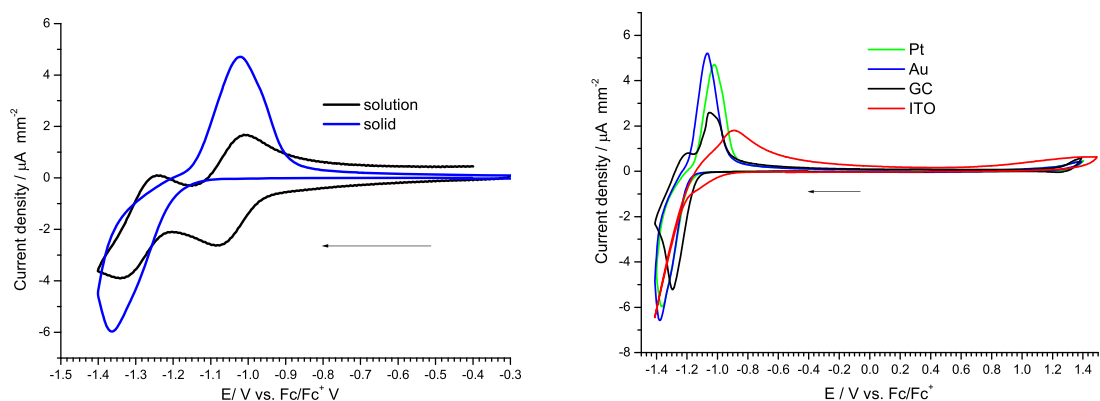


Fig. 9. Selected cyclic voltammograms obtained for **2**. Reduction (left on GC electrode) and on various electrode (right), arrow shows the initial direction of current flow; $c = 10^{-5} \text{ mol/dm}^3$, sweep rate $\nu = 100 \text{ mV/s}$, $0.1 \text{ M Bu}_4\text{NPF}_6$ in CH_2Cl_2 .

(or p-doping) after the oxidation the layer in direct contact with the surface of the electrode the further flow of the charge is considerably limited. However, during a similar situation when the reduction is performed, electrons are more easily transported into

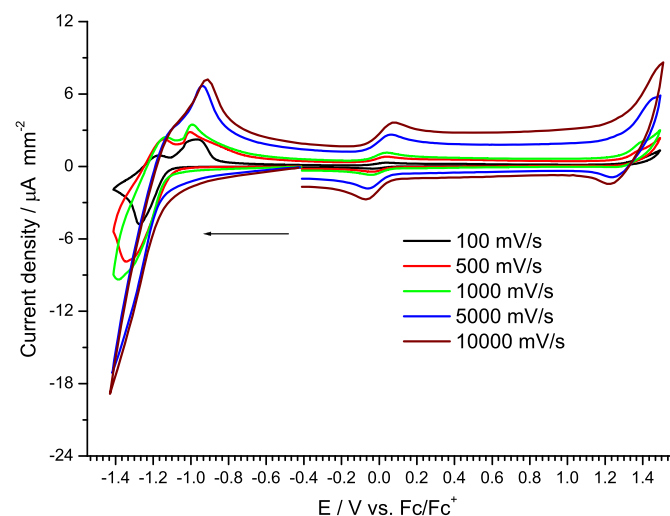


Fig. 10. Cyclic voltammograms obtained for **2** at different scan rate (as solid on GC electrode), arrow shows the initial direction of current flow; $c = 10^{-5} \text{ mol/dm}^3$, $0.1 \text{ M Bu}_4\text{NPF}_6$ in CH_2Cl_2 .

a solid. Thus, in solid state work function is rather determined (instead of IE or HOMO level).

We have also investigated the influence of scan rate. As can be seen at Fig. 10 at higher scan rate band gap determined from peak onset is slightly lowered. On the other hand, at higher scan rate peak onset is more pronounced (especially when we look at oxidation for **2**) (similar as observed by C. Yang et al. [29]). Previously, we have also reported in details the influence of pH [30], type of acid [31] or nanoparticles [32] on optical and electrochemical properties. Additionally, very recently M. Pasini et al. have shown that the CV response may be also affected by the used electrolyte [33].

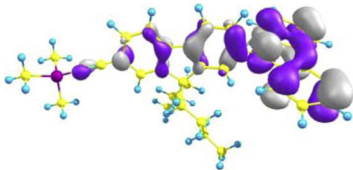
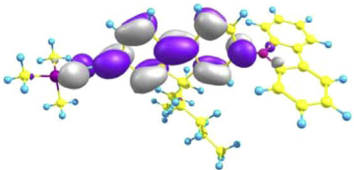
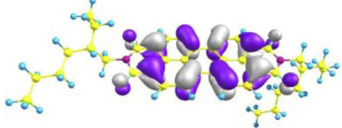
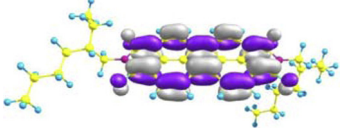
Finally, we have compared experimental data with DFT calculations (see Table 1) using equation:

$$IE(eV) = |e|(E_{\text{ox(onset)}} + 5.1) \text{ and } EA(eV) = -|e|(E_{\text{red(onset)}} + 5.1) \quad [7]$$

As can be seen in Table 2 in case of **1** HOMO is laying on both aromatic moieties with small contribution from acetylene group. On the other hand, LUMO is located only at fluorine and acetylene part of molecule. For **2** both HOMO and LUMO are located exclusively on polycyclic aromatic moieties. However, in both cases H/L transition is allowed.

In both cases band gap determined for diluted solutions by UV-vis spectroscopy is higher than those from cyclic voltammetry technique (230 mV for **1** and 160 mV for **2**). It is probably caused by previously mentioned additional hole-electron binding energy. Additionally, in **2** HOMO and LUMO are located in the same

Table 2
HOMO, LUMO contours of the **1** and **2** compounds.

	HOMO	LUMO
1		
2	 E = -5.79 eV	 E = -1.86 eV
	 E = -6.14 eV	 E = -3.68 eV

molecule region, while for **1** they are partially separated – it could causing difficulties in electron transfer (some energy is consumed for electron transport within molecule). However, both band gap values determined experimentally are significantly lower than calculated from $\text{HOMO}_{(\text{DFT})} - \text{LUMO}_{(\text{DFT})}$, which is a common observation [1,25]. It is worth noting when we use $|\text{IE}| - |\text{EA}|$ formula, is in the better agreement with experimentally one (see Table 1). But still, calculation in each case lowered the energy level for about 0.3 eV approximately, what is also commonly obtained result [28,34,35]. Thus, DFT is a helpful tool, allowing deeper photophysical properties understanding, however they must be used with caution.

4. CONCLUSIONS

To summarize, we carried out NMR, CV and UV–vis spectroscopy studies (with the aid of DFT calculations) of the selected semiconducting PDI and carbazole derivatives. We have observed that working electrode type influence must be considered, especially when there is possibility of chemical surface-compounds interaction or during the measurement of multistep reduction/oxidation. Additionally, concentration of measured species is crucial for obtained value estimation. We have also observed that NMR spectra obtained at various concentrations can be used to estimate intermolecular interaction degree. In the case of small interaction (**1**) differences between value obtained for solution and solid state are small. However, when interactions are strong (**2**) differences are significant. Our study also revealed that theoretically determined band gap from $|\text{IP}| - |\text{EA}|$ equation better fits to experimental data than determined from HOMO–LUMO equation. However, DFT overestimated IE and EA value, which needs further investigation. Generally, many variables mentioned above affected the resulted value, thus in each cases all experimental conditions should be precisely defined in order to be repeated or compared with data from different source.

Acknowledgments

This work was supported by National Science Centre of Poland Grant No. DEC-2015/17/N/ST5/03892 and NCBiR Grant No. PBS2/A5/40/2014. Calculations have been carried out in Wroclaw Centre for Networking and Supercomputing (<http://www.wcss.pl>), grant No. 18.

Appendix A. Supplementary data

Supplementary data associated with this article can be found, in the online version, at <http://dx.doi.org/10.1016/j.electacta.2016.09.046>.

References

- [1] M.C. Ruiz Delgado, E.-G. Kim, D.A. da Silva Filho, J.-L. Bredas, Tuning the Charge-Transport Parameters of Perylene Diimide Single Crystals via End and/or Core Functionalization: A Density Functional Theory Investigation, *J. Am. Chem. Soc.* 132 (2010) 3375–3387, doi:<http://dx.doi.org/10.1021/ja908173x>.
- [2] A. Tomkeviciene, J.V. Grazulevicius, D. Volyniuk, V. Jankauskas, G. Sini, Structure?properties relationship of carbazole and fluorene hybrid trimers: experimental and theoretical approaches, *Phys Chem Chem Phys* 16 (2014) 13932–13942, doi:<http://dx.doi.org/10.1039/C4CP00302K>.
- [3] N. Sakai, J. Mareda, E. Vauthey, S. Matile, Core-substituted naphthalenediimides, *Chem. Commun.* 46 (2010) 4225–4237, doi:<http://dx.doi.org/10.1039/C0CC00078G>.
- [4] M. Grucela-Zajac, M. Filapek, L. Skorka, J. Gasiorowski, E.D. Glowacki, H. Neugebauer, E. Schab-Balcerzak, Thermal, optical, electrochemical, and electrochromic characteristics of novel polyimides bearing the Acridine Yellow moiety, *Mater. Chem. Phys.* 137 (2012) 221–234, doi:<http://dx.doi.org/10.1016/j.matchemphys.2012.09.011>.
- [5] S.S. Naghavi, T. Gruhn, V. Aljani, G.H. Fecher, C. Felser, K. Medjanik, D. Kutnyakhov, S.A. Nepijko, G. Schönhense, R. Rieger, M. Baumgarten, K. Müllen, Theoretical study of new acceptor and donor molecules based on polycyclic aromatic hydrocarbons, *J. Mol. Spectrosc.* 265 (2011) 95–101, doi:<http://dx.doi.org/10.1016/j.jms.2010.12.004>.
- [6] C. Arantes, M. Scholz, R. Schmidt, V. Dehm, M.L.M. Rocco, A. Schöll, F. Reinert, F. Würthner, Comparative analysis of the energy levels of planar and core-twisted perylene bisimides in solution and solid state by UV/VIS, CV, and UPS/IPES, *Appl Phys A* 108 (2012) 629–637, doi:<http://dx.doi.org/10.1007/s00339-012-6941-3>.
- [7] R. Rybakiewicz, P. Gawrys, D. Tsikritzis, K. Emmanouil, S. Kennou, M. Zagorska, A. Pron, Electronic properties of semiconducting naphthalene bisimide derivatives—Ultraviolet photoelectron spectroscopy versus electrochemistry, *Electrochim. Acta* 96 (2013) 13–17, doi:<http://dx.doi.org/10.1016/j.electacta.2013.02.041>.
- [8] J.-L. Bredas, Mind the gap!, *Mater. Horiz.* 1 (2014) 17–19, doi:<http://dx.doi.org/10.1039/C3MH00098B>.
- [9] P. Bujak, I. Kulszewicz-Bajer, M. Zagorska, V. Maurel, I. Wielgus, A. Pron, Polymers for electronics and spintronics, *Chem. Soc. Rev.* 42 (2013) 8895–8999, doi:<http://dx.doi.org/10.1039/C3CS60257E>.
- [10] A. Pron, P. Gawrys, M. Zagorska, D. Djurado, R. Demadrille, Electroactive materials for organic electronics: preparation strategies, structural aspects and characterization techniques, *Chem. Soc. Rev.* 39 (2010) 2577–2632, doi:<http://dx.doi.org/10.1039/B907999H>.
- [11] C.M. Cardona, W. Li, A.E. Kaifer, D. Stockdale, G.C. Bazan, Electrochemical Considerations for Determining Absolute Frontier Orbital Energy Levels of Conjugated Polymers for Solar Cell Applications, *Adv. Mater.* 23 (2011) 2367–2371, doi:<http://dx.doi.org/10.1002/adma.201004554>.
- [12] W. Yue, Y. Zhao, H. Tian, D. Song, Z. Xie, D. Yan, Y. Geng, F. Wang, Poly (oligothiophene-alt-benzothiadiazole)s: Tuning the Structures of

- Oligothiophene Units toward High-Mobility Black Conjugated Polymers, *Macromolecules* 42 (2009) 6510–6518, doi:<http://dx.doi.org/10.1021/ma900906t>.
- [13] C.-W. Chang, H.-Y. Tsai, K.-Y. Chen, Green Perylene Bisimide Dyes: Synthesis, Photophysical and Electrochemical Properties, *Materials* 7 (2014) 5488–5506, doi:<http://dx.doi.org/10.3390/ma7085488>.
- [14] S.H. Lee, T. Nakamura, T. Tsutsui, Synthesis and Characterization of Oligo(9,9-dihexyl-2,7-fluorene ethynylene)s: For Application as Blue Light-Emitting Diode, *Org. Lett.* 3 (2001) 2005–2007, doi:<http://dx.doi.org/10.1021/ol010069r>.
- [15] X. Ma, E.A. Azeem, X. Liu, Y. Cheng, C. Zhu, Synthesis and tunable chiroptical properties of chiral BODIPY-based π -conjugated polymers, *J Mater Chem C* 2 (2014) 1076–1084, doi:<http://dx.doi.org/10.1039/C3TC32029D>.
- [16] Y. Lin, Y. Chen, T.-L. Ye, Z.-K. Chen, Y.-F. Dai, D.-G. Ma, Oligofluorene-based push-pull type functional materials for blue light-emitting diodes, *J. Photoch. Photobio. A* 230 (2012) 55–64, doi:<http://dx.doi.org/10.1016/j.jphotochem.2011.12.008>.
- [17] Y. Wang, L. Zhang, G. Zhang, Y. Wu, S. Wu, J. Yu, L. Wang, A new colorimetric and fluorescent bifunctional probe for Cu^{2+} and F^- ions based on perylene bisimide derivatives, *Tetrahedron Lett.* 55 (2014) 3218–3222, doi:<http://dx.doi.org/10.1016/j.tetlet.2014.03.137>.
- [18] W. Wang, L.-S. Li, G. Helms, H.-H. Zhou, A.D.Q. Li, To Fold or to Assemble?, *J. Am. Chem. Soc.* 125 (2003) 1120–1121, doi:<http://dx.doi.org/10.1021/ja027186h>.
- [19] P.-O. Schwartz, L. Biniek, E. Zaborova, B. Heinrich, M. Brinkmann, N. Leclerc, S. Méry, Perylenebisimide-Based Donor–Acceptor Dyads and Triads: Impact of Molecular Architecture on Self-Assembling Properties, *J. Am. Chem. Soc.* 136 (2014) 5981–5992, doi:<http://dx.doi.org/10.1021/ja4129108>.
- [20] M. Grucela-Zajac, M. Filapek, L. Skorka, K. Bijak, K. Smolarek, S. Mackowski, E. Schab-Balcerzak, Photophysical, electrochemical and thermal properties of new (co)polyimides incorporating oxadiazole moieties, *Synthetic Met.* 188 (2014) 161–174, doi:<http://dx.doi.org/10.1016/j.synthmet.2013.12.012>.
- [21] Y.-C. Kung, S.-H. Hsiao, Solution-processable, high- T_g , ambipolar polyimide electrochromics bearing pyrenylamine units, *J. Mater. Chem.* 21 (2011) 1746–1754, doi:<http://dx.doi.org/10.1039/C0JM02642E>.
- [22] K. Bijak, M. Filapek, M. Wiacek, H. Janeczek, M. Grucela, K. Smolarek, S. Mackowski *Mater. Chem. Phys.* 171 (2016) 97–108, doi:<http://dx.doi.org/10.1016/j.matchemphys.2015.12.005c>.
- [23] M. Grucela-Zajac, K. Bijak, S. Kula, M. Filapek, M. Wiacek, H. Janeczek, L. Skorka, J. Gasiorowski, K. Hingerl, N.S. Sariciftci, N. Nosidlak, G. Lewinska, J. Sanetra, E. Schab-Balcerzak, (Photo)physical Properties of New Molecular Glasses End-Capped with Thiophene Rings Composed of Diimide and Imine Units, *J. Chem. Phys. C* 118 (2014) 13070–13086, doi:<http://dx.doi.org/10.1021/jp501168b>.
- [24] P. Gawrys, A. Zoltowska, M. Zagorska, A. Pron, Alternating copolymers of oligoarylenes and naphthalene bisimides as low band gap semiconductors: Synthesis, electrochemical and spectroelectrochemical behavior, *Electrochimica Acta* 56 (2011) 10464–10472, doi:<http://dx.doi.org/10.1016/j.electacta.2011.03.016>.
- [25] M. Czichy, P. Wagner, L. Grządziel, M. Krzywiecki, A. Sz wajca, M. Łapkowski, J. Zak, D.L. Officer, Electrochemical and photoelectronic studies on C60-pyrrolidine- functionalised poly(terthiophene), *Electrochimica Acta* 141 (2014) 51–60, doi:<http://dx.doi.org/10.1016/j.electacta.2014.06.100>.
- [26] A.O. Aleshinloye, J.B. Bodapati, H. Icil, Synthesis, characterization, optical and electrochemical properties of a new chiral multichromophoric system based on perylene and naphthalene diimides, *J. Photoch. Photobio. A* 300 (2015) 27–37, doi:<http://dx.doi.org/10.1016/j.jphotochem.2014.12.007>.
- [27] E. Kozma, D. Kotowski, M. Catellani, S. Luzzati, A. Famulari, F. Bertini, Synthesis and characterization of new electron acceptor perylene diimide molecules for photovoltaic applications, *Dyes Pigments* 99 (2013) 329–338, doi:<http://dx.doi.org/10.1016/j.dyepig.2013.05.011>.
- [28] J. Vura-Weis, M.A. Ratner, M.R. Wasielewski, Geometry and Electronic Coupling in Perylenebisimide Stacks: Mapping Structure-Charge Transport Relationships, *J. Am. Chem. Soc.* 132 (2010) 1738–1739, doi:<http://dx.doi.org/10.1021/ja907761e>.
- [29] C. Yang, A. Tang, X. Li, K. Jiang, F. Teng, Electrochemical evaluation of the frontier orbitals of organic dyes in aqueous electrolyte, *Electrochimica Acta* 102 (2013) 108–112, doi:<http://dx.doi.org/10.1016/j.electacta.2013.04.005>.
- [30] A. Iwan, B. Boharewicz, I. Tazbir, M. Filapek, Enhanced power conversion efficiency in bulk heterojunction solar cell based on new polyazomethine with vinylene moieties and [6,6]-phenyl C_{61} butyric acid methyl ester by adding 10-camphorsulfonic acid, *Electrochimica Acta* 159 (2015) 81–92, doi:<http://dx.doi.org/10.1016/j.electacta.2015.01.215>.
- [31] A. Iwan, M. Palewicz, I. Tazbir, B. Boharewicz, R. Pietruszka, M. Filapek, J. Wojtkiewicz, B.S. Witkowski, F. Graneł, M. Godlewski, Influence of $\text{ZnO}:\text{Al}$, MoO_3 and PEDOT:PSS on efficiency in standard and inverted polymer solar cells based on polyazomethine and poly(3-hexylthiophene), *Electrochimica Acta* 191 (2016) 784–794, doi:<http://dx.doi.org/10.1016/j.electacta.2016.01.107>.
- [32] A. Iwan, B. Boharewicz, I. Tazbir, M. Filapek, K.P. Korona, P. Wróbel, T. Stefaniuk, A. Ciesielski, J. Wojtkiewicz, A.A. Wronkowska, A. Wronkowski, B. Zboromirska-Wnukiewicz, S. Grankowska-Ciechanowicz, M. Kaminska, T. Szoplík, How do 10-camphorsulfonic acid, silver or aluminum nanoparticles influence optical, electrochemical, electrochromic and photovoltaic properties of air and thermally stable triphenylamine-based polyazomethine with carbazole moieties? *Electrochimica Acta* 185 (2015) 198–210, doi:<http://dx.doi.org/10.1016/j.electacta.2015.10.110>.
- [33] M. Pasini, B. Vercellib, G. Zotti, A. Berlin, Solid-state Effects in the Cyclic Voltammetric HOMO–LUMO Determination: The case of Dinitrophenyl-hydrazone a, ν -substituted Oligothiophenes, *Electrochimica Acta* 193 (2016) 261–267, doi:<http://dx.doi.org/10.1016/j.electacta.2016.02.035>.
- [34] A. Szłapa, S. Kula, U. Błaszczewicz, M. Grucela, E. Schab-Balcerzak, M. Filapek, Simple donor– π -acceptor derivatives exhibiting aggregation-induced emission characteristics for use as emitting layer in OLED, *Dyes and Pigments* 129 (2016) 80–89, doi:<http://dx.doi.org/10.1016/j.dyepig.2016.02.002>.
- [35] S.A. Kula Szłapa, J.G. Malecki, A. Maron, M. Matussek, E. Schab-Balcerzak, M. Siwy, M. Domanski, M. Sojka, W. Danikiewicz, S. Krompiec, M. Filapek, Synthesis and photophysical properties of novel multisubstituted benzene and naphthalene derivatives with high 2D- π -conjugation, *Optical Materials* 47 (2015) 118–128, doi:<http://dx.doi.org/10.1016/j.optmat.2015.07.011>.